

# The Unified Transform for a Reaction-Diffusion Brain Tumor Model that Incorporates Tissue Heterogeneity and Radiotherapy

A.G. Sifalakis, M.G. Papadomanolaki, E.P. Papadopoulou and Y.G. Saridakis

**Abstract**—Gliomas are primary brain tumors characterized by rapid growth and aggressive diffusive behavior. Radiation therapy, following extensive surgical resection, is included among the standard protocols for the treatment of this kind of malignant tumors. Several mathematical models have been developed to approximate the evolution of gliomas. In this paper we consider a linear reaction-diffusion tumor growth problem in  $1 + 1$  dimensions that, except from the heterogeneity of the brain tissue, takes into consideration the effect of radiotherapy treatment. Extending recent results, our main objective is, by utilizing the unified transform, to obtain an integral representation of the solution that also incorporates the effect of radiotherapy. Among several advantages of the unified transform is the fact that one may recover the value of the solution at any point  $(x, t)$  directly, without prior knowledge of the solution at any previous time level other than the initial. Simple trapezoidal rule on appropriate hyperbolic contours leads to efficient numerical evaluation of the integral representation.

**Keywords**—Gliomas, Radiotherapy, Reaction-Diffusion PDEs, Fokas Unified Transform, Numerical Integration.

## I. INTRODUCTION

**G**LIOMAS, one of the most common and aggressive forms of primary brain tumors, are well known for their rapid growth and highly diffuse invasion of adjacent normal tissue. To study the core properties of motile glioma cells, namely migration and proliferation, mathematical models (cf. e.g. [3], [5], [20], [23]; for a review see also [13], [11] and [10]) considered reaction-diffusion PDEs and, based on CT-scan data, calculated the values of the diffusion and proliferation parameters. Brain's tissue heterogeneity (gray and white matter) was incorporated later in the basic model by making use of a properly discontinuous diffusion coefficient (cf. [18], [19]).

Recently, in [15], [16] and [4], the model was further extended to also incorporate the effects of radiotherapy as, combined with surgery and chemotherapy, it is considered to be a standard treatment regime.

The unified transform, a new method for solving linear and integrable nonlinear PDEs, was introduced in [6]- [7], and since then has been studied and further developed by many researchers (see [8] for a review). The method is characterized

Manuscript received June 15, 2015; revised July 10, 2015.

This work was supported by the ESF and Greek national funds through the operational program *Education and Lifelong Learning* of the National Strategic Reference Framework (NSRF) THALES (Grant number: MIS-379416).

All authors are with the Applied Mathematics & Computers Laboratory, Technical University of Crete, 73100 Chania, Crete, Greece

Email of the corresponding author : y.saridakis@amcl.tuc.gr

by novel integral representations of the solution in the complex  $k$ -plane which are uniformly convergent and, via contour deformation, decay exponentially.

The implementation of the unified transform method for brain tumor models with discontinuous diffusion coefficient was introduced in [12] and further studied in [1] and [2]. Our main objective of the present work is to further extend our results on the unified transform method to include also heterogeneous brain tumor models that incorporate the effect of radiotherapy. Our results refer on the  $1 + 1$  dimensions case as the work for higher dimensions is still in progress.

## II. METHODOLOGY

### A. Mathematical model

Assuming exponential tumor growth and a simple log-kill radiotherapy model, the core reaction-diffusion PDE of the mathematical model, considered here, takes the form (cf. [19], [16], [15]):

$$\frac{\partial \bar{c}}{\partial \bar{t}} = \nabla \cdot (\bar{D} \nabla \bar{c}) + \bar{\rho} \bar{c} - \bar{R}(\bar{t}) \bar{c}, \quad (1)$$

where  $\bar{c}(\bar{x}, \bar{t})$  denotes the tumor cell density at location  $\bar{x} \in \mathbb{R}^n$  ( $n = 1, 2, 3$ ) and time  $\bar{t}$ ,  $\bar{\rho}$  stands for the net proliferation rate (cf. [3]),  $\bar{D}$  is the diffusion coefficient representing the active motility of malignant cells (cf. [20]) and  $\bar{R}(\bar{t})$  describes the effect of radiotherapy. The dimensions of the above variables are:

$$\begin{cases} [\bar{x}] = cm, & [\bar{t}] = day, & [\bar{c}] = \frac{cells}{cm^n}, \\ [\bar{D}] = \frac{cm^2}{day}, & [\bar{\rho}] = \frac{1}{day}, & [\bar{R}] = \frac{1}{day} \end{cases} \quad (2)$$

At the boundary we consider zero flux, which impose no migration of cells beyond the brain boundaries, and an initial condition  $\bar{c}(\bar{x}, 0) = \bar{f}(\bar{x})$ , where  $\bar{f}(\bar{x})$  is the initial spatial distribution of malignant cells.

Due to the heterogeneity of the brain tissue the diffusion coefficient  $\bar{D}$  is defined by (cf. [18], [19]):

$$\bar{D} \equiv \bar{D}(\bar{x}) = \begin{cases} D_w, & \bar{x} \text{ in white matter } (\bar{x} \in \bar{\Omega}_w) \\ D_g, & \bar{x} \text{ in gray matter } (\bar{x} \in \bar{\Omega}_g) \end{cases}, \quad (3)$$

where  $D_w$  and  $D_g$  are scalars with  $D_w > D_g$ .

Considering a low-dose-rate and fractionated radiotherapy, activated in the time interval  $(\bar{T}_G, \bar{T}_R]$ , the effect of radiotherapy is described by (cf. [15]):

$$\bar{R} \equiv \bar{R}(\bar{t}) = R_{\text{eff}} k_R(\bar{t}), \quad (4)$$

where  $k_R(\bar{t})$  denotes the temporal profile of the radiation schedule and, by using a time step of one day, takes the value one on the radiotherapy days and zero otherwise, that is

$$k_R(\bar{t}) = \begin{cases} 1, & \bar{t} \in (\bar{T}_G, \bar{T}_R] \\ 0, & \bar{t} \notin (\bar{T}_G, \bar{T}_R] \end{cases}. \quad (5)$$

$R_{\text{eff}}$  denotes the effect of  $n$  fractions of radiation per day and is described by (cf. [15] and the references therein)

$$R_{\text{eff}} = \alpha(nd) + 2\beta nd^2 \left[ g(\mu\tau) + 2 \frac{\cosh(\mu\tau) - 1}{(\mu\tau)^2} h_n(\phi) \right],$$

with

$$g(\mu\tau) = \frac{\mu\tau - 1 + e^{-\mu\tau}}{(\mu\tau)^2} \text{ and } h_n(\phi) = \frac{(n-1-n\phi+\phi^n)\phi}{n(1-\phi)^2}$$

where  $\alpha, \beta$  are sensitivity parameters,  $d$  is the dose rate at time  $\bar{t}$ ,  $\mu$  is the half time for repair of radiation-induced DNA damage,  $\tau$  is the irradiation duration and  $\phi = e^{-\mu(\tau+\Delta\tau)}$  with  $\Delta\tau$  denoting the time interval between fractions. We point out that the values of the parameters used in all the above relations may be found, for example, in [15] (see the list of parameter values included in Table 1 of [15] and the corresponding references therein).

Working towards the direction of describing the model problem in  $(\bar{x}, \bar{t})$  regions where  $\bar{c}$  may be considered analytic inside and continuous on the boundary, let us first define  $\bar{c}$  on three consecutive time regions  $\bar{t}_\ell$ ,  $\ell = 1, 2, 3$  as follows:

$$\begin{cases} \bar{c}(\bar{x}, \bar{t}_1) = \bar{c}(\bar{x}, \bar{t}) & , \quad \bar{t} \in (0, \bar{T}_G] \\ \bar{c}(\bar{x}, \bar{t}_2) = \bar{c}(\bar{x}, \bar{t} - \bar{T}_G) & , \quad \bar{t} \in (\bar{T}_G, \bar{T}_R] \\ \bar{c}(\bar{x}, \bar{t}_3) = \bar{c}(\bar{x}, \bar{t} - \bar{T}_R) & , \quad \bar{t} \in (\bar{T}_R, \bar{T}_F] \end{cases}. \quad (6)$$

Using, now, the above notation, the model problem in 1+1 dimensions is written as:

$$\begin{cases} \frac{\partial \bar{c}}{\partial \bar{t}_\ell} = (\bar{D} \bar{c}_{\bar{x}})_{\bar{x}} + \bar{\rho}_\ell \bar{c}, & \bar{x} \in [\bar{a}, \bar{b}], \quad 0 < \bar{t}_\ell \leq \bar{T}_\ell \\ \bar{c}(\bar{x}, 0) = \bar{c}_\ell(\bar{x}) & \\ \bar{c}_{\bar{x}}(\bar{a}, \bar{t}_\ell) = \bar{c}_{\bar{x}}(\bar{b}, \bar{t}_\ell) = 0 & \end{cases}. \quad (7)$$

where

$$\begin{cases} \bar{\rho}_1 = \bar{\rho} & , \quad \bar{T}_1 = \bar{T}_G & , \quad \bar{c}_1(\bar{x}) = \bar{f}(\bar{x}) \\ \bar{\rho}_2 = \bar{\rho} - R_{\text{eff}} & , \quad \bar{T}_2 = \bar{T}_R - \bar{T}_G & , \quad \bar{c}_2(\bar{x}) = \bar{c}(\bar{x}, \bar{T}_1) \\ \bar{\rho}_3 = \bar{\rho} & , \quad \bar{T}_3 = \bar{T}_F - \bar{T}_R & , \quad \bar{c}_3(\bar{x}) = \bar{c}(\bar{x}, \bar{T}_2) \end{cases}. \quad (8)$$

## B. Dimensionless Variables and Equivalence Transformations

The dimensionless form of the IBVPs in (7) is given by

$$\begin{cases} \frac{\partial c}{\partial t_\ell} = (D c_x)_x + \rho_\ell c, & x \in [a, b], \quad 0 < t_\ell \leq T_\ell \\ c(x, 0) = c_\ell(x) & \\ c_x(a, t_\ell) = c_x(b, t_\ell) = 0 & \end{cases} \quad (9)$$

where (cf. [18], [2])

$$\begin{cases} x = \chi \bar{x}, \quad a = \chi \bar{a}, \quad b = \chi \bar{b}, \quad t_\ell = \bar{\rho} \bar{t}_\ell, \\ c(x, t_\ell) = \frac{1}{\chi N_0} \bar{c}(\chi \bar{x}, \bar{\rho} \bar{t}_\ell) \\ c_\ell(x) = \frac{1}{\chi N_0} \bar{c}_\ell(\chi \bar{x}) \\ D = \frac{\bar{D}}{D_w}, \quad \rho_\ell = \frac{\bar{\rho}_\ell}{\bar{\rho}} \end{cases} \quad (10)$$

with

$$x = \sqrt{\frac{\bar{\rho}}{D_w}} \text{ and } N_0 = \int_{\bar{a}}^{\bar{b}} \bar{f}(\bar{x}) d\bar{x}, \quad (11)$$

and, obviously,  $T_j = \bar{\rho} \bar{T}_j$ . Also, observe that  $N_0$  denotes the initial number of glioma cells in  $[\bar{a}, \bar{b}]$ .

Furthermore, upon immediate application of the corresponding result in [2], we also have that:

**Lemma 1.** If  $c(x, t_\ell)$ ,  $\ell = 1, 2, 3$  satisfies the IBVP in (9)-(11) and  $u(x, t_\ell)$  is defined by

$$u(x, t_\ell) = e^{-\rho_\ell t_\ell} c(x, t_\ell), \quad (12)$$

then  $u(x, t_\ell)$ ,  $\ell = 1, 2, 3$  satisfies the IBVP

$$\begin{cases} \frac{\partial u}{\partial t_\ell} = (D u_x)_x, & x \in [a, b], \quad 0 < t_\ell \leq T_\ell \\ u(x, 0) = u_\ell(x) \equiv c_\ell(x) & \\ u_x(a, t_\ell) = u_x(b, t_\ell) = 0 & \end{cases}. \quad (13)$$

## C. The Unified Transform

To proceed, now, with the application of the Unified Transform for the solution of the IBVPs in (13), let us first fix notation with brain's heterogeneity regions of white  $\Omega_w$  and gray  $\Omega_g$  matter inside the interval  $[a, b]$ . Namely, as in [2], we shall consider  $[a, b]$  partitioned into  $n + 1$  sub-intervals  $R_j := (w_{j-1}, w_j)$ , with  $a \equiv w_0 < w_1 < w_2 < \dots < w_n < w_{n+1} \equiv b$ , and if  $R_j \subseteq \Omega_w$ , for some  $j$ , then  $R_{j-1} \subseteq \Omega_g$  and  $R_{j+1} \subseteq \Omega_g$ . With this notation, the diffusion coefficient  $D$ , defined in (10), takes the form

$$D(x) = \gamma_j = \begin{cases} \gamma, & \text{when } x \in \Omega_g \\ 1, & \text{when } x \in \Omega_w \end{cases}, \quad (14)$$

where  $\gamma = D_g/D_w$ . As, now, the parabolic nature of the problem directly implies continuity of both  $u$  and  $Du_x$  across

each interface point  $w_j$ , for each  $j = 1, 2, \dots, n$  and  $\ell = 1, 2, 3$ , there holds

$$\begin{cases} \lim_{x \rightarrow w_j^+} u(x, t_\ell) = \lim_{x \rightarrow w_j^-} u(x, t_\ell) \\ \lim_{x \rightarrow w_j^+} D(x)u_x(x, t_\ell) = \lim_{x \rightarrow w_j^-} D(x)u_x(x, t_\ell) \end{cases}. \quad (15)$$

Let  $u^{(j)}(x, t_\ell)$  denote the solution of the problem defined in Lemma 1 over the region  $[w_{j-1}, w_j] \times [0, T_\ell]$ . Observing that its analyticity and continuity properties in the interior and on the boundaries on this region allow Green's and Cauchy's theorems to be applied, immediate application of our analysis in [2] implies:

**Proposition 1.** *If  $u^{(j)}(x, t_\ell)$ , for each  $j = 1, 2, \dots, n$  and  $\ell = 1, 2, 3$ , denotes the solution of the IBVP defined in Lemma 1 over the region  $[w_{j-1}, w_j] \times [0, T_\ell]$  and  $k \in \mathbb{C}$ , then*

$$\begin{aligned} u^{(j)}(x, t_\ell) &= \frac{c_j}{2\pi} \int_{-\infty}^{+\infty} e^{ic_j kx - k^2 t_\ell} \tilde{u}_\ell^{(j)}(c_j k) dk \\ &\quad - \frac{1}{2\pi c_j} \int_{\partial\Gamma^+} e^{ic_j k(x-w_{j-1}) - k^2 t_\ell} \\ &\quad \cdot [\tilde{u}_x^{(j)}(w_{j-1}, k^2) + ic_j k \tilde{u}^{(j)}(w_{j-1}, k^2)] dk \\ &\quad - \frac{1}{2\pi c_j} \int_{\partial\Gamma^-} e^{ic_j k(x-w_j) - k^2 t_\ell} \\ &\quad \cdot [\tilde{u}_x^{(j)}(w_j, k^2) + ic_j k \tilde{u}^{(j)}(w_j, k^2)] dk, \end{aligned} \quad (16)$$

where

- $c_j = 1/\sqrt{\gamma_j}$
- $\Gamma^+$  and  $\Gamma^-$  denote the contours (see also Fig. 1)

$$\Gamma^+ = \{k \in \mathbb{C} : \arg(k) \in (\frac{\pi}{4}, \frac{3\pi}{4})\},$$

$$\Gamma^- = \{k \in \mathbb{C} : \arg(k) \in (\frac{5\pi}{4}, \frac{7\pi}{4})\},$$

- $u_\ell^{(j)}(x)$  are the initial data, defined in Lemma 1, restrained over region  $[w_{j-1}, w_j]$ , and  $\tilde{u}_\ell^{(j)}(x)$  denotes its Fourier transform, defined by

$$\tilde{u}_\ell^{(j)}(k) = \int_{w_{j-1}}^{w_j} e^{-ikx} u_\ell^{(j)}(x) dx. \quad (17)$$

The quantities  $\tilde{u}^{(j)}$  and  $\tilde{u}_x^{(j)}$  are given by the solution of the  $(2n+2) \times (2n+2)$  complex linear system

$$GU = F, \quad (18)$$

where the nonzero elements of the matrix  $G = \{G_{p,q}\}$  are defined by:

- for  $j = 1$ :

$$\begin{bmatrix} G_{1,1} & G_{1,2} & G_{1,3} \\ G_{2,1} & G_{2,2} & G_{2,3} \end{bmatrix} = \begin{bmatrix} A_1^{(1)} & A_3^{(1)} & A_4^{(1)} \\ A_5^{(1)} & A_7^{(1)} & A_8^{(1)} \end{bmatrix} \quad (19)$$

- for  $j = 2, 3, \dots, n$ :

$$\begin{aligned} &\begin{bmatrix} G_{2j-1,2j-2} & G_{2j-1,2j-1} & G_{2j-1,2j} & G_{2j-1,2j+1} \\ G_{2j,2j-2} & G_{2j,2j-1} & G_{2j,2j} & G_{2j,2j+1} \end{bmatrix} = \\ &= \begin{bmatrix} A_1^{(j)} & A_2^{(j)} & A_3^{(j)} & A_4^{(j)} \\ A_5^{(j)} & A_6^{(j)} & A_7^{(j)} & A_8^{(j)} \end{bmatrix} \end{aligned} \quad (20)$$

- for  $j = n+1$ :

$$\begin{aligned} &\begin{bmatrix} G_{2n+1,2n} & G_{2n+1,2n+1} & G_{2n+1,2n+2} \\ G_{2n+2,2n} & G_{2n+2,2n+1} & G_{2n+2,2n+2} \end{bmatrix} = \\ &= \begin{bmatrix} A_1^{(n+1)} & A_2^{(n+1)} & A_3^{(n+1)} \\ A_5^{(n+1)} & A_6^{(n+1)} & A_7^{(n+1)} \end{bmatrix} \end{aligned} \quad (21)$$

with

$m$	$A_m^{(j)}$	$A_{m+1}^{(j)}$
1	$ic_j \gamma_j k e^{-ic_j k w_{j-1}}$	$\gamma_{j-1} e^{-ic_j k w_{j-1}}$
3	$-ic_j \gamma_j k e^{-ic_j k w_j}$	$-\gamma_j e^{-ic_j k w_j}$
5	$-ic_j \gamma_j k e^{ic_j k w_{j-1}}$	$\gamma_{j-1} e^{ic_j k w_{j-1}}$
7	$ic_j \gamma_j k e^{ic_j k w_j}$	$-\gamma_j e^{ic_j k w_j}$

and

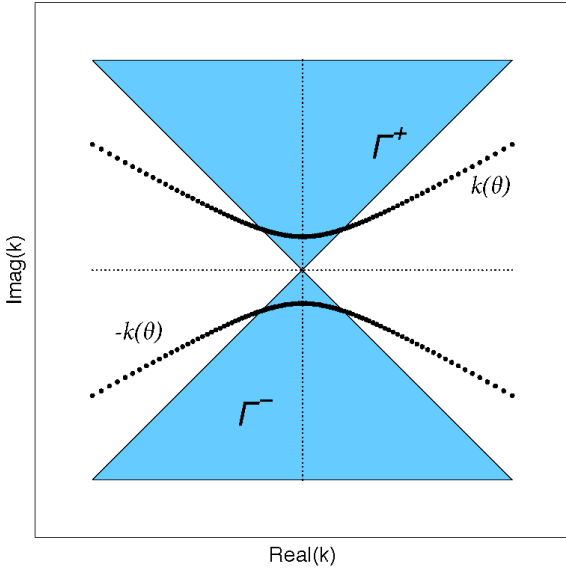
$$U = \begin{bmatrix} \tilde{u}^{(1)}(a, k^2) \\ \tilde{u}^{(1)}(w_1, k^2) \\ \tilde{u}_x^{(1)}(w_1, k^2) \\ \vdots \\ \tilde{u}^{(n)}(w_n, k^2) \\ \tilde{u}_x^{(n)}(w_n, k^2) \\ \tilde{u}^{(n+1)}(b, k^2) \end{bmatrix}, \quad F = \begin{bmatrix} \hat{f}^{(1)}(c_1 k) \\ \hat{f}^{(1)}(-c_1 k) \\ \vdots \\ \hat{f}^{(n+1)}(c_{n+1} k) \\ \hat{f}^{(n+1)}(-c_{n+1} k) \end{bmatrix}.$$

#### D. Numerical Integration Contours and Integral Properties

It is known (cf. [21], [22]; see also [9], [14], [2]) that for the efficient numerical evaluation of the above integrals in (16) one may apply the trapezoid rule on suitable hyperbolic contours. For this, we deform (cf. e.g. [2]) the integration paths  $\partial\Gamma^\pm$  to hyperbolae of the complex plane by the mapping:

$$k_\theta \equiv k(\theta) := i \sin(\beta - i\theta), \quad (22)$$

where the angle  $\beta$  is chosen to be  $\beta = \pi/6$  and the curves  $\pm k(\theta)$  are shown schematically in Fig. 1 that follows.

Fig. 1: The contours  $\pm k(\theta)$  for numerical integration

The above mapping leads us in rewriting the solution (16) as

$$\begin{aligned} u_\ell^{(j)}(x, t_\ell) = & \frac{c_j}{2\pi} \int_{-\infty}^{+\infty} e^{ic_j k x - k^2 t_\ell} \hat{u}_\ell^{(j)}(c_j k) dk \\ & - \frac{1}{2\pi c_j} \int_{-\infty}^{+\infty} e^{ic_j k_\theta(x - w_{j-1}) - k_\theta^2 t_\ell} \\ & \cdot [\tilde{u}_x^{(j)}(w_{j-1}, k_\theta^2) + ic_j k_\theta \tilde{u}^{(j)}(w_{j-1}, k_\theta^2)] k'_\theta dk_\theta \\ & - \frac{1}{2\pi c_j} \int_{-\infty}^{+\infty} e^{-ic_j k_\theta(x - w_j) - k_\theta^2 t_\ell} \\ & \cdot [\tilde{u}_x^{(j)}(w_j, k_\theta^2) - ic_j k_\theta \tilde{u}^{(j)}(w_j, k_\theta^2)] k'_\theta dk_\theta, \end{aligned} \quad (23)$$

where  $k'_\theta$  denotes the derivative of  $k(\theta)$ .

For the efficient implementation of the numerical quadrature rules - in particular for the evaluation of the last two integrals - one has to take into consideration (cf. [2] for example) basic algebraic properties such as:

- The real parts of the integrands are *even* functions of  $\theta$ .
- The imaginary parts of the integrands are *odd* functions of  $\theta$ .
- The integrands are decaying functions of  $\theta$ .

Application of the above properties directly implies that

$$\int_{-\infty}^{\infty} U(\theta) d\theta = 2 \int_0^{\infty} \operatorname{Re}(U(\theta)) d\theta \approx 2 \int_0^{\Theta} \operatorname{Re}(U(\theta)) d\theta,$$

where  $U(\theta)$  denotes any one of the last two integrands involved in (23) and  $\Theta$  is a relatively *small* real number. For a good estimate of  $\Theta$  one may require the dominant exponential term  $e^{-k_\theta^2 \tau}$ , common in all integrals, to satisfy

$$\left| e^{-k_\theta^2 \tau} \right| \leq 10^{-M} \text{ for all } \theta \geq \Theta \equiv \Theta(\tau; M)$$

for sufficiently large  $M$ , hence (cf. [12])

$$\Theta = \frac{1}{2} \ln \frac{4\tau + 8M \ln 10}{\tau}. \quad (24)$$

### III. NUMERICAL EXPERIMENTS

Two different numerical experiments are included in this section to visually demonstrate the behavior of their semi-analytical solution by an effective combination of the unified transform and numerical quadrature rules on hyperbolic contours. We would like to clarify that said model problems are virtual cases and have no relevance with real patient data.

The per day radiotherapy protocol, followed in both models, is identical. Namely, we assumed that the administered per day radiation dose is  $d = 1.8\text{Gy}$  and, by using the parameter values (cf. [15])  $\alpha = 0.027$ ,  $\beta = 0.0027$ ,  $n = 1$ ,  $\mu = 11.4$ ,  $\tau = 0.0083$ ,  $\Delta\tau = 1$ , the radiation coefficient in both models satisfies  $R_{\text{eff}} = 0.05707849$ .

#### A. Model Problem I

Referring to the model problem in (7), consider the values:

$$\begin{cases} \bar{a} = -10 \text{ cm}, \bar{b} = 10 \text{ cm}, \bar{w}_1 = -5 \text{ cm}, \bar{w}_2 = 5 \text{ cm} \\ \bar{\Omega}_g = [\bar{a}, \bar{w}_1] \cup (\bar{w}_2, \bar{b}] \text{ and } \bar{\Omega}_w = [\bar{w}_1, \bar{w}_2] \\ D_g = 0.0013 \text{ cm}^2\text{day}^{-1}, D_w = 0.0065 \text{ cm}^2\text{day}^{-1} \\ \bar{\rho} = 0.012 \text{ day}^{-1}, N_0 = 100 \text{ cells} \end{cases} \quad (25)$$

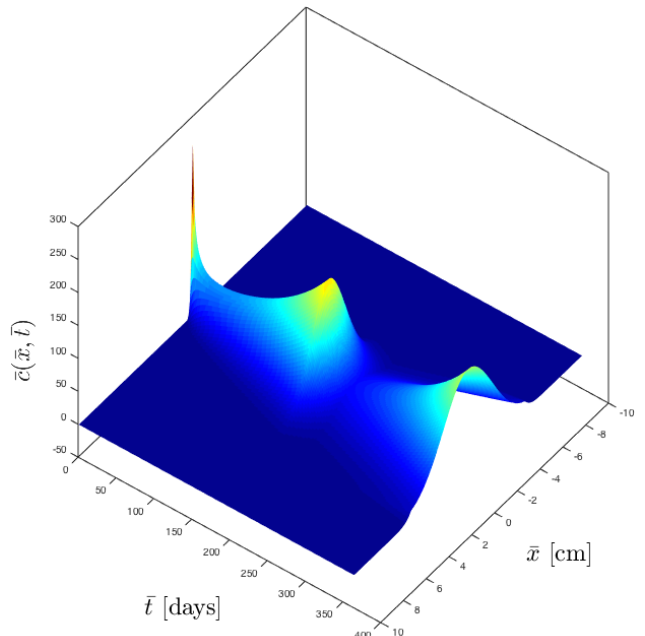
The initial distribution of cells is considered to be

$$\bar{f}(\bar{x}) = N_0 \delta(\bar{x}),$$

where  $\delta(\bar{x})$  denotes Dirac's delta.

We considered a radiotherapy period of 35 days, started on  $\bar{T}_G = 180$  day and finished on  $\bar{T}_R = 215$  day, during which the total administered radiation dose is 63Gy.

The results from applying a simple trapezoidal rule, using 50 quadrature points, for the evaluation of each one of the integrals in relation (23) are depicted in Fig. 2 and Fig. 3.

Fig. 2: Time evolution of the cell density  $\bar{c}(\bar{x}, \bar{t})$  for one glioma cell source. Radiotherapy period of 35 days (from 180 to 215).

More specifically, in Fig. 2, the evolution of the cell density function  $\bar{c}(\bar{x}, \bar{t})$  is depicted for a total period of  $\bar{T}_F = 365$  days. By inspection, one may easily recognize the time periods the tumor grows without treatment, hence diffusion and proliferation dominate, as well as the time period of radiotherapy.

The radiotherapy effect on the total number of tumor cells  $N(\bar{t})$ , defined by

$$N(\bar{t}) = \int_{\bar{a}}^{\bar{b}} \bar{c}(\bar{x}, \bar{t}) d\bar{x},$$

is depicted in Fig. 3. The differential between treated and untreated tumor growth reveals that the administered radiotherapy extended survival by 166 days.

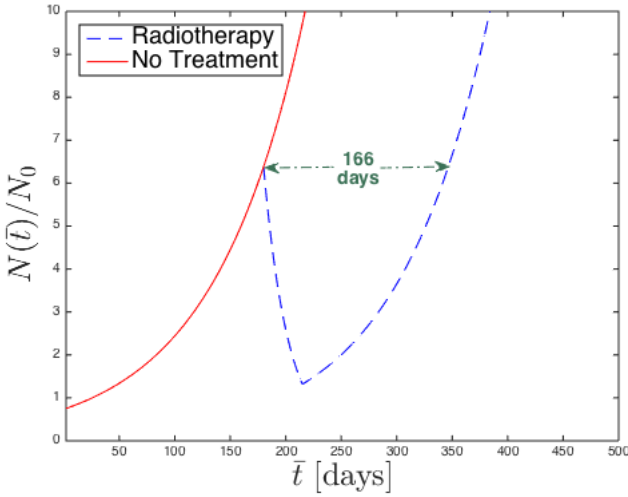


Fig. 3: The effect of radiotherapy on the total number of tumor cells.

### B. Model Problem II

In this problem we consider four initial point sources of malignant cells. Referring, again, to the model problem in (7), we consider the values:

$$\left\{ \begin{array}{l} \bar{a} = -10 \text{ cm}, \bar{b} = 10 \text{ cm} \\ \bar{w}_1 = -6 \text{ cm}, \bar{w}_2 = -5 \text{ cm}, \bar{w}_3 = 1 \text{ cm}, \bar{w}_4 = 7 \text{ cm} \\ \bar{\Omega}_g = [\bar{a}, \bar{w}_1] \cup (\bar{w}_2, \bar{w}_3) \cup (\bar{w}_4, \bar{b}] \\ \bar{\Omega}_w = [\bar{w}_1, \bar{w}_2] \cup [\bar{w}_3, \bar{w}_4] \\ D_g = 0.0013 \text{ cm}^2 \text{day}^{-1}, D_w = 0.0065 \text{ cm}^2 \text{day}^{-1} \\ \bar{\rho} = 0.012 \text{ day}^{-1}, N_0 = 400 \text{ cells} \end{array} \right. \quad (26)$$

and the initial distribution of tumor cells is given by

$$\bar{f}(\bar{x}) = \frac{N_0}{4} [\delta(\bar{x} + 8) + \delta(\bar{x} + 3) + \delta(\bar{x} - 4) + \delta(\bar{x} - 6)].$$

We implemented a radiotherapy period of 40 days, started on  $\bar{T}_G = 180$  day and finished on  $\bar{T}_R = 220$  day, during which the total administered radiation dose is 72Gy.

The results from applying a trapezoidal rule, using 50 quadrature points, for the evaluation of each one of the integrals in relation (23) are depicted in Fig. 4 and Fig. 5.

As in model problem I, Fig. 4 depicts the evolution of the cell density function  $\bar{c}(\bar{x}, \bar{t})$  for a total period of  $\bar{T}_F = 365$  days. Again, the time periods the tumor grows without treatment as well as the time period of radiotherapy are easily recognizable.

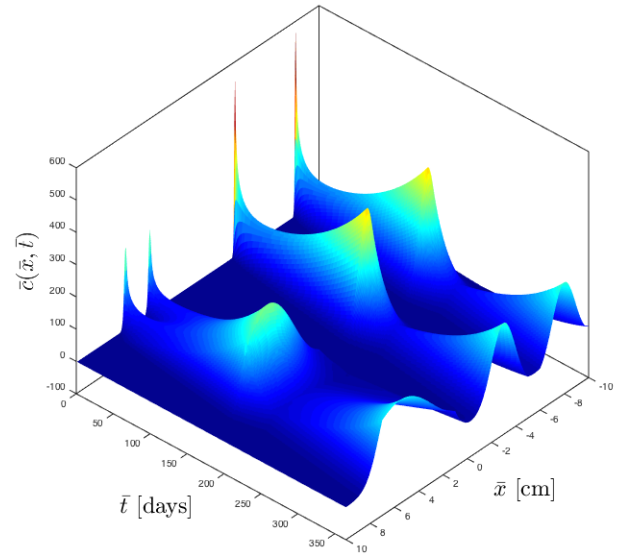


Fig. 4: Time evolution of the cell density  $\bar{c}(\bar{x}, \bar{t})$  for four glioma cell sources. Radiotherapy period of 40 days (from 180 to 220).

The radiotherapy effect on the total number of tumor cells  $N(\bar{t})$  is depicted in Fig. 5. The differential between treated and untreated tumor growth reveals that the administered radiotherapy extended survival by 190 days.

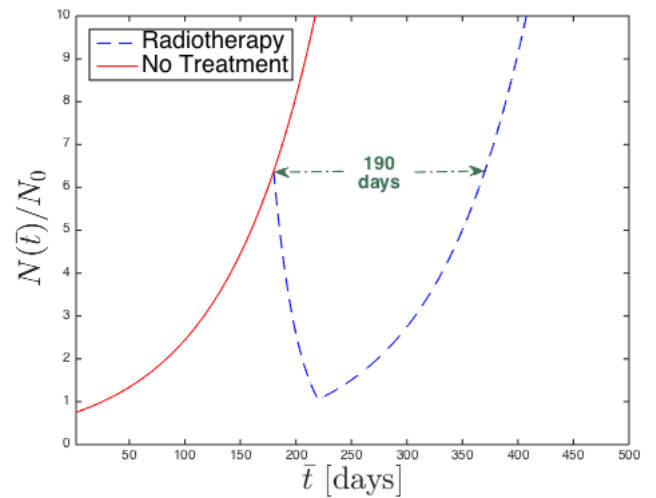


Fig. 5: The effect of radiotherapy on the total number of tumor cells.

### IV. CONCLUSIONS

In the present work, extending recently produced results (cf. [12], [1], [2]), we used the Unified Transform, as well as the trapezoidal rule on hyperbolic contours, to derive and evaluate novel integral representations of a linear reaction-diffusion

problem's solution that models the growth of aggressive brain tumors, in a heterogeneous environment, and incorporates the effect of radiotherapy. The results, although limited to the 1+1 dimension case, reveal the potential of the method to describe exactly the solution at any space-time point without depending on any other data apart from the initial data of all stages. And this, not only for domains that solutions remain smooth, but for multi-domain environments that include discontinuities of the solution's partial derivatives not only in space but in time as well, as we showed here. In this way we clearly enlight the path to effectively solve more general models that incorporate surgical resection and chemotherapy as well, and, of course, contribute to the solution of the problem in 2+1 dimensions.

#### ACKNOWLEDGEMENT

The present research work has been co-financed by the European Union (European Social Fund ESF) and Greek national funds through the Operational Program Education and Lifelong Learning of the National Strategic Reference Framework (NSRF) - Research Funding Program: THALES (Grant number: MIS-379416). Investing in knowledge society through the European Social Fund.

#### REFERENCES

- [1] M. Asvestas, A. G. Sifalakis, E.P. Papadopoulou and Y. G. Saridakis, *Fokas method for a multi-domain linear reaction-diffusion equation with discontinuous diffusivity*, IOP Science Journal of Physics: Conference Series, 490, 012143, 2014.
- [2] M. Asvestas, E.P. Papadopoulou, A. G. Sifalakis and Y. G. Saridakis,, *The Unified Transform for a Class of Reaction-Diffusion Problems with Discontinuous Time Dependent Parameters*, Proceedings of the World Congress on Engineering 2015.
- [3] J. Cook, D. E. Woodward, P. Tracqui and J. D. Murray, *Resection of gliomas and life expectancy*, J Neurooncol., 24, 131, 1995.
- [4] D. Corwin, C. Holdsworth, R. C. Rockne, An. D. Trister, M. M. Mrugala, J. K. Rockhill, R. D. Stewart2, M. Phillips2 and K. R. Swanson, *Toward Patient-Specific, Biologically Optimized Radiation Therapy Plans for the Treatment of Glioblastoma*, PLOS ONE, 8(11), 1-9, 2013.
- [5] G.C. Cruywagen, D.E. Woodward, P. Tracqui, G.T. Bartoo, J.D. Murray and E.C. Alvord Jr, *The modeling of diffusive tumors*, Journal of Biological Systems , vol.3, pp.937-945, 1995.
- [6] A. S. Fokas, *A unified transform method for solving linear and certain nonlinear PDEs*, Proc.R.Soc. A, 453, 1411-1443, 1997.
- [7] A. S. Fokas, *A new transform method for evolution PDEs*, IMA J. Appl. Math.,67(6), 559-590, 2002.
- [8] A. S. Fokas, *A Unified Approach to Boundary Value Problems*, SIAM, Philadelphia, 2008.
- [9] N. Flyer and A. S. Fokas, *A hybrid analytical-numerical method for solving evolution partial differential equations I: The half-line*, Proc. R. Soc. A, 464, 1823-1849, 2008.
- [10] H. L. P. Harpold, E. C. Alvord Jr and K. R. Swanson, *The Evolution of Mathematical Modeling of Glioma Proliferation and Invasion*, J Neuropathol Exp Neurol, 66(1), 1-9, 2007.
- [11] U. Ledzewicz, H. Schittler, A. Friedman and E. Kashdan, *Mathematical Methods and Models in Biomedicine*, Springer Science and Business Media, 2012.
- [12] D. Mantzaftos, M. G. Papadomanolaki, Y. G. Saridakis and A. G. Sifalakis, *Fokas transform method for a brain tumor invasion model with heterogeneous diffusion in 1+1 dimensions*, Applied Numerical Mathematics (<http://dx.doi.org/10.1016/j.apnum.2014.09.006>), 2014.
- [13] J.D. Murray, *Mathematical Biology I and II*, Springer-Verlag, 3rd Edition 2002.
- [14] T.S. Papatheodorou and A. N. Kandili, *Novel numerical techniques based on Fokas transforms, for the solution of initial boundary value problems*, Journal of Computational and Applied Mathematics 227:75-82, 2009.
- [15] G. Powathil, M. Kohandel, S. Sivaloganathan, A. Oza and M. Milosevic, *Mathematical modeling of brain tumors: effects of radiotherapy and chemotherapy*, Phys. Med. Biol. 52 :3291-3306, 2007.
- [16] R. Rockne, E. C. Alvord Jr., J. K. Rockhill and K. R. Swanson, *A mathematical model for brain tumor response to radiation therapy*, J. Math. Biol., 58, 561578, 2009.
- [17] D.A. Smith, *Well-posed two-point initial-boundary value problems with arbitrary boundary conditions*, Math. Proc. Camb. Philos. Soc. 152:473496, 2012.
- [18] K. R. Swanson, *Mathematical modeling of the growth and control of tumors*, PHD Thesis, University of Washington, 1999.
- [19] K. R. Swanson, E. C. Alvord Jr and J. D. Murray, *A quantitative model for differential motility of gliomas in grey and white matter*, Cell Proliferation, 33, 317-329, 2000.
- [20] P. Tracqui, G. C. Cruywagen, D. E. Woodward, T. Bartoo, J.D. Murray and E. C. Alvord Jr, *A mathematical model of glioma growth: the effect of chemotherapy on spatio-temporal growth*, Cell Prolif, 28 1731, 1995.
- [21] L. N. Trefethen, J. A. C. Weideman and T. Schmelzer, *Tablot quadratures and rational approximations*, BIT Numerical Mathematics, 46:653-670, 2006.
- [22] J. A. C. Weideman and L. N. Trefethen, *Parabolic and hyperbolic contours for computing the bromwich integral*, Math. Comp., 76(259), 13411356, 2007.
- [23] D. E. Woodward, J. Cook, P. Tracqui, G. C. Cruywagen, J. D. Murray and E. C. Alvord Jr, *A mathematical model of glioma growth: the effect of extent of surgical resection*, Cell Proliferation, vol.29, pp.269-288, 1996.